Food and Chemical Toxicology 133 (2019) 110761

Contents lists available at ScienceDirect

Food and Chemical Toxicology

journal homepage: www.elsevier.com/locate/foodchemtox

Protein kinase Cδ mediates methamphetamine-induced dopaminergic neurotoxicity in mice *via* activation of microsomal epoxide hydrolase

Eun-Joo Shin[a,1], Ji Hoon Jeong[b,1], Garima Sharma[a], Naveen Sharma[a], Dae-Joong Kim[c], Duc Toan Pham[a], Quynh Dieu Trinh[a], Duy-Khanh Dang[d], Seung-Yeol Nah[e], Guoying Bing[f], Hyoung-Chun Kim[a,*]

[a] Neuropsychopharmacology and Toxicology Program, College of Pharmacy, Kangwon National University, Chunchon, 24341, Republic of Korea
[b] Department of Pharmacology, College of Medicine, Chung-Ang University, Seoul, 06974, Republic of Korea
[c] Department of Anatomy and Cell Biology, Medical School, Kangwon National University, Chunchon, 24341, Republic of Korea
[d] Pharmacy Faculty, Can Tho University of Medicine and Pharmacy, Can Tho City, 900000, Viet Nam
[e] Ginsentology Research Laboratory and Department of Physiology, College of Veterinary Medicine, KonKuk University, Seoul, 05029, Republic of Korea
[f] Department of Neuroscience, College of Medicine, University of Kentucky, Lexington, KY, 40536, USA

ARTICLE INFO

Keywords:
Methamphetamine
Dopamine
PKCδ knockout mice
mEH knockout mice
Proapoptosis
Oxidative stress

ABSTRACT

We previously demonstrated that activation of protein kinase Cδ (PKCδ) is critical for methamphetamine (MA)-induced dopaminergic toxicity. It was recognized that microsomal epoxide hydrolase (mEH) also induces dopaminergic neurotoxicity. It was demonstrated that inhibition of PKC modulates the expression of mEH. We investigated whether MA-induced PKCδ activation requires mEH induction in mice. MA treatment (8 mg/kg, i.p., × 4; 2 h interval) significantly enhanced the level of phosphorylated PKCδ in the striatum of wild type (WT) mice. Subsequently, treatment with MA resulted in significant increases in the expression of cleaved PKCδ and mEH. Treatment with MA resulted in enhanced interaction between PKCδ and mEH. PKCδ knockout mice exhibited significant attenuation of the enhanced mEH expression induced by MA. MA-induced hyperthermia, oxidative stress, proapoptotic potentials, and dopaminergic impairments were attenuated by PKCδ knockout or mEH knockout in mice. However, treating mEH knockout in mice with PKCδ inhibitor, rottlerin did not show any additive beneficial effects, indicating that mEH is a critical mediator of neurotoxic potential of PKCδ. Our results suggest that MA-induced PKCδ activation requires mEH induction as a downstream signaling pathway and that the modulation of the PKCδ and mEH interaction is important for the pharmacological intervention against MA-induced dopaminergic neurotoxicity.

1. Introduction

Protein kinase C (PKC) is a superfamily of isozymes that play diverse roles in the regulation of cellular processes, such as proliferation, pro-inflammation, and differentiation (Giorgi et al., 2010). Among the PKC family members PKCδ is known to plays a critical role in regulating the inflammation, oxidative stress, and proapoptosis (Yoshida, 2007; Mai et al., 2018a, 2018b; Shin et al., 2018a, 2019). As PKCδ is highly expressed in the brain (Naik et al., 2000), it has been implicated in various physiological and pathophysiological processes of the central nervous system. Previously, we demonstrated that treatment with MA does not significantly alter the expression of PKCα, PKCβI, PKCβII, or PKCζ in the striatum, but significantly enhances the expression of PKCδ (Shin et al., 2012, 2017). We also reported that gene knockout or pharmacological inhibition of PKCδ attenuates the MA-induced hyperthermia, oxidative stress, and dopaminergic impairments (Nguyen et al., 2015; Shin et al., 2011, 2012, 2014, 2017, 2018a).

Further, we suggested that PKCδ promotes MA-induced dopaminergic neurodegeneration by inhibiting the phosphorylation of tyrosine hydroxylase (TH) (Shin et al., 2011, 2012). It is recognized that phosphorylation of TH can be regulated by dephosphorylation reaction, such as, protein phosphatase 2A (PP2A), a major serine/threonine phosphatase that dephosphorylates TH, resulting in reduced TH activity (Haavik et al., 1989; Zhang et al., 2007b). We demonstrated that MA treatment promotes dephosphorylation of TH-Ser^{40} via inducing striatal PP2A activity (Dang et al., 2015). In addition, genetic or

* Corresponding author.
E-mail address: kimhc@kangwon.ac.kr (H.-C. Kim).
[1] The first two authors contributed equally to this work.

https://doi.org/10.1016/j.fct.2019.110761
Received 12 May 2019; Received in revised form 9 August 2019; Accepted 13 August 2019
Available online 15 August 2019

pharmacological inhibition of PKCδ attenuated the MA-induced increase in PP2A activity, resulting in increased phosphorylation of TH-Ser^{40} and TH activity (Dang et al., 2015), suggesting that induction of TH activity requires the phosphorylation.

The central nervous system (CNS) can be a potential target for xenobiotics. Hence, xenobiotic detoxification mechanisms are required for the protection of the CNS. The cytochrome P450 (CYP) system and microsomal epoxide hydrolase (mEH) are important for the biotransformation of xenobiotics. The CYP system and mEH are expressed in multiple organs, including brain (Fretland and Omiecinski, 2000; Omiecinski et al., 2000). The CYP can generate unstable and chemically reactive endogenous epoxides. A recent study suggested a functional interaction between mEH and CYP system (Orjuela Leon et al., 2017). CYP isozyme is known to participate in MA metabolism (Cherner et al., 2010). MA is thermally degraded to *trans*-phenylpropene, which may follow CYP-catalyzed biotransformation pathway, to yield an epoxide intermediate (Melnick, 2002). Although mEH plays an important role in the detoxification of epoxide intermediate, it may also result in the generation of toxic by-products. However, very little is known about the role of mEH in dopaminergic neurotoxicity induced by MA. In this study, we used PKCδ knockout and mEH knockout mice to investigate the modulation of the PKCδ and mEH interaction in the dopaminergic neurotoxicity induced by MA. Finally, we propose that the interaction between PKCδ and mEH is critical for promoting MA-induced dopaminergic neurotoxicity.

2. Materials and methods

2.1. Experimental design

The experimental design of this study is shown in Fig. 1. All mice were treated in accordance with the NIH Guide for the Humane Care and Use of Laboratory Animals. All mice were maintained on a 12/12-h light/dark cycle and fed *ad libitum*. The mice were allowed to adapt to these conditions for 2 weeks before the experiment.

2.2. Development and characterization of PKCδ knockout and mEH knockout mice

The PKCδ knockout mice have been previously described (Dang et al., 2018b; Mai et al., 2018a, 2019a; Shin et al., 2016; Tran et al., 2018b). A breeding pair of PKCδ heterozygous mice, originally bred into a C57BL/6 J background, was a gift from Dr. K. I. Nakayama (Dept. of Molecular Genetics, Medical Institute of Bioregulation, Kyushu University, Fukuoka, Japan) (Miyamoto et al., 2002). All the mice were subsequently maintained and bred into the C57BL6/J background for at least nine generations in a specific pathogen-free (SPF) facility before use with wild-type (WT) mice from the same litter in our experiments. The tail DNA was evaluated to genotype WT and PKCδ knockout mice. Further details on the genetic characterization are described in the Supplementary materials and methods.

The mEH knockout mice have been previously described (Liu et al., 2008). The mEH knockout mice were derived from a breeding stock provided by Frank J. Gonzalez at the National Institutes of Health (Miyata et al., 1999). The strain was back crossed at least nine times to the C57BL/6 J background. For studies with mEH knockout, WT littermates were used as controls. The tail DNA was evaluated to genotype WT and mEH knockout mice. Further details on the genetic characterization of mice are described in the Supplementary materials and methods.

2.3. Drug treatment

Eight-week-old WT, PKCδ knockout, and mEH knockout mice received four doses of MA (8 mg/kg, i.p.) or saline at 2 h intervals (Fig. 1A and B), because binge MA injection is traditional tool for inducing dopaminergic toxicity (Omonijo et al., 2014; Beauvais et al., 2011; Liu et al., 2013; Shin et al., 2012; Dang et al., 2017a; Nguyen et al., 2015).

It was demonstrated that the lack of endogenous melatonin in C57BL/6 J mice is based on very low enzymatic activity of arylalkylamine N-acetyltransferase (AANAT) (Ebihara et al., 1986; Goto et al., 1994), due to a severely truncated AANAT protein (Roseboom et al., 1998). Our previous results (Nguyen et al., 2015) are in agreement with those obtained by Yu et al. (2002), who reported that C57BL/6 J mice treated with MA during the light cycle and dark cycle show comparable striatal dopamine levels. Similarly, we previously demonstrated that the circadian cycle (i.e., light or dark phase) does not significantly affect MA-induced dopaminergic changes and locomotor activity in both WT and PKCδ knockout mice (Nguyen et al., 2015). Thus, we raise the possibility that a negligible effect of endogenous melatonin of MA-induced dopaminergic neurotoxicity may be due to the fact that C57BL/6 J mouse shows an extremely low level of melatonin secretion (Roseboom et al., 1998). Therefore, it is plausible that PKCδ knockout and mEH knockout mice are not sensitive to circadian cycle, because their background is derived from C57BL/6 J.

The PKCδ inhibitor rottlerin (Biomol Research Laboratories Inc., Plymouth, PA, USA) was dissolved in dimethyl sulfoxide (DMSO) as a stock solution, and stored at −20 °C. Rottlerin was diluted in sterile saline immediately before use. The mEH knockout mice were pretreated with rottlerin (10 mg/kg, i.p.) once a day for 5 days. On day 6, mEH knockout mice received four doses of MA (8 mg/kg, i.p.) or saline at 2 h intervals (Fig. 1C). Two additional treatments with rottlerin (10 mg/kg, i.p.) were performed at 4 h and 0.5 h before the first MA injection. The dose of rottlerin was determined based on a previous study (Zhang et al., 2007a). Mice were euthanized over a period of time after final MA treatment to examine biochemical and histological changes in the brain of mice. Mice were anesthetized with sodium pentobarbital (60 mg/kg, i.p.; Sigma-Aldrich, St. Louis, MO, USA) and euthanized by cervical dislocation and brain was removed (Mai et al., 2018c).

2.4. Measuring rectal temperature

The rectal temperature (under ambient temperature: 21 ± 1 °C) was measured by inserting a thermometer probe lubricated with oil at least 3 cm into the rectum of mice. To prevent sudden movements, animals were gently handled with a woolen glove while their tail was moved to allow probe insertion. This was done to reduce any effect of restraint stress on the rectal temperature. When the attempt to insert the probe was not successful (due to sudden movement of the animal or the need to restrain the mouse), the animal was excluded from the group (Nguyen et al., 2018; Shin et al., 2011; Tran et al., 2019).

2.5. Western blot analysis

Striatal tissues were lysed in buffer containing a 200 mM Tris–HCl (pH 6.8), 1% SDS, 5 mM ethylene glycol-bis (2-aminoethyl ether)-N, N, N′, N′-tetraacetic acid (EGTA), 5 mM EDTA, 10% glycerol, 1 × phosphatase inhibitor cocktail I (Sigma-Aldrich, St. Louis, MO, USA), and 1 × protease inhibitor cocktail (Sigma-Aldrich). Lysate was centrifuged at 12,000 × *g* for 30 min, and the supernatant fraction was utilized for western blot analysis as described previously. The protein was quantified using the BCA protein assay reagent (Thermo Scientific, Rockford, IL, USA). Biotechnology). The proteins (20 μg/lane) were resolved by SDS polyacrylamide gel electrophoresis (SDS-PAGE) using 8 or 10% gel. The proteins were then transferred onto a polyvinylidene fluoride (PVDF) membranes. The membrane was pre-incubated with 5% non-fat milk for 30 min followed by incubation overnight at 4 °C with primary antibody against PKCδ (1:1000; Santa Cruz Biotechnology), cleaved-PKCδ (1:1000; Santa Cruz Biotechnology), phospho-PKCδ (p-PKCδ) at Tyr311 (1:500; Santa Cruz Biotechnology), mEH (1:1000; Santa Cruz Biotechnology), Bax (1:1000; Santa Cruz), cleaved caspase-3 (1:1000; Cell Signaling Technology, Inc., Danvers, MA, USA), caspase-3 (1:5000;

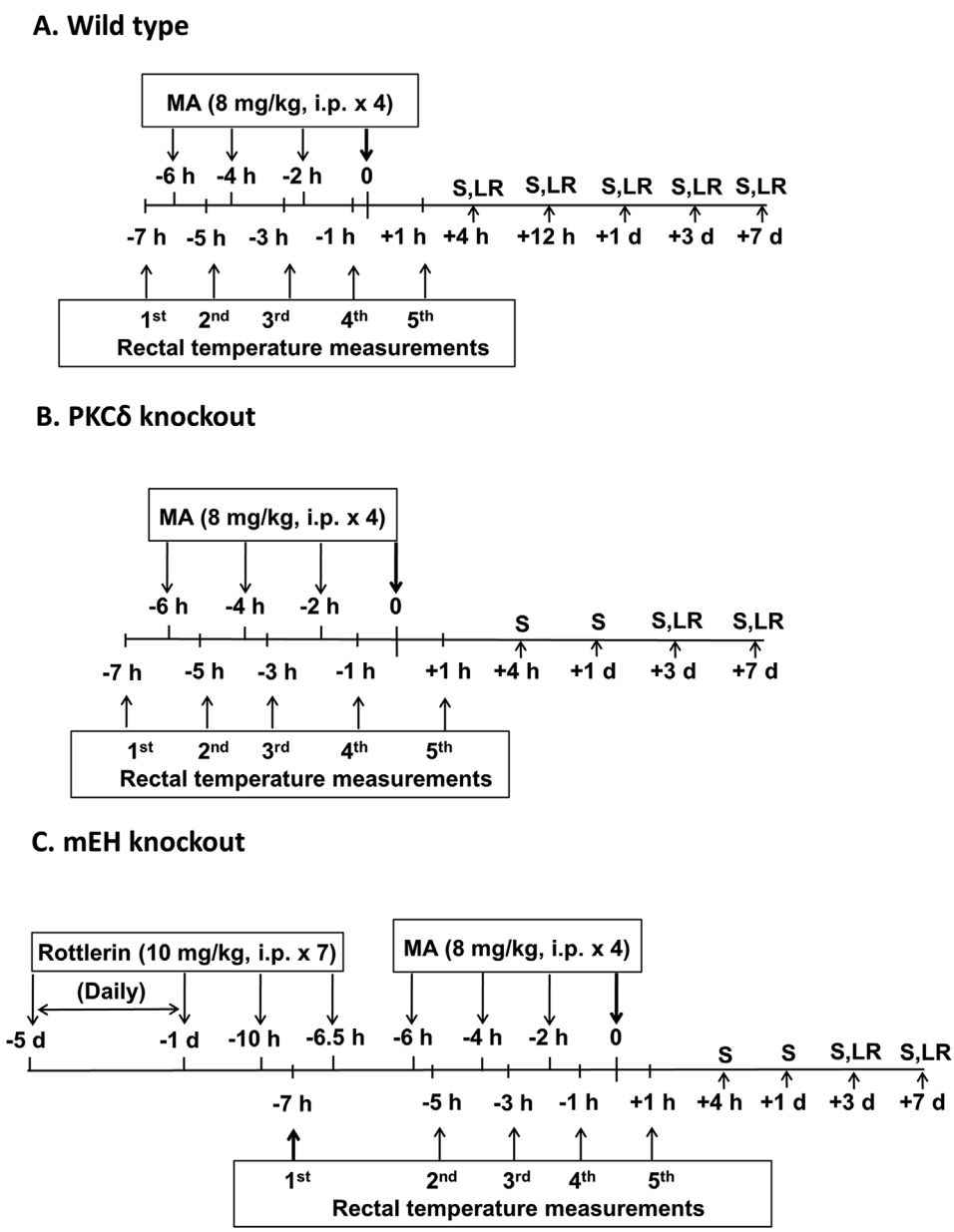

Fig. 1. Experimental design for elucidating the interaction between protein kinase Cδ (PKCδ) and microsomal epoxide hydrolase (mEH) in methamphetamine (MA)-induced dopaminergic toxicity in mice. Wild type (WT) mice received MA (8 mg/kg, i.p., 4 doses at 2 h interval) or saline. Basal rectal temperature (RT) was measured 1 h before the first MA administration. In addition, RT was measured 1 h before every MA treatment. Behavioral changes (locomotor activity and rotarod performance) were assessed at 4 h, 12 h, 1 d, 3 d and 7 d after the final MA injection. Mice were sacrificed immediately after the behavioral assessments to examine neurochemical parameters (A). WT and PKCδ knockout mice received MA (8 mg/kg, i.p., 4 doses at 2 h interval) or saline. Behavioral changes were measured at 4 h, 1 d, 3 d, and 7 d after the final MA treatment. Mice were sacrificed immediately after the behavioral assessments days 3 and 7 after the final MA treatment to examine neurochemical parameters (B). mEH knockout mice received rottlerin (10 mg/kg, i.p.), once a day for five consecutive days, and at 4 h and 30 min before the first MA injection. Behavioral assessments (i.e., locomotor activity and rotarod performance) were performed at 4 h, 1 d, 3 d, and 7 d after the final MA treatment. Mice were sacrificed immediately after the behavioral assessments at days 3 and 7 after the final MA treatment to examine neurochemical parameters (C). S = sacrifice; LR = locomotor activity/rotarod performance.

Cell Signaling Technology, Inc.), Bcl-2 (1:1000; Santa Cruz Biotechnology), Bcl-xL (1:1000; Cell Signaling Technology, Inc.), TH (1:5000; Chemicon, EMD Millipore), or β-actin (1:50000; Sigma-Aldrich). Western blot assay was performed as described previously (Mai et al., 2019a; Nguyen et al., 2018). The PVDF membranes were then incubated with horseradish peroxidase (HRP)-conjugated secondary anti-rabbit IgG (1:1000; GE Healthcare, Piscataway, NJ, USA), anti-mouse IgG (1:1000; Sigma), or anti-goat IgG (1:1000; Sigma) antibody for 2 h. The membrane was visualized using the ECL plus® enhanced chemiluminescence system (GE Healthcare). The relative band intensities were quantified using PhotoCapt MW (version 10.01 for Windows; Vilber Lourmat, Marne la Vallée, France), and then normalized to β-actin intensity.

2.6. Immunoprecipitation

Immunoprecipitation was performed as described previously (Dang et al., 2017a; Tran et al., 2018a, 2019) using protein G-sepharose (GE Healthcare, Piscataway, NJ, U.S.A.). The striatal tissue were homogenized in lysis buffer for 1 min on ice and centrifuged at 12,000 × *g* for 20 min at 4 °C to remove the particulate matter. The supernatant fraction was transferred to fresh tubes in 1 mL aliquots and pre-cleared by the addition of 50 μL of protein G-sepharose suspension (GE Healthcare) to each tube. The tubes were gently mixed for 1 h at 4 °C, and centrifuged at 12,000 × *g* for 20 s. Five hundred microliter aliquot of the pre-cleared supernatant fraction was then transferred to fresh tubes and incubated with 2 μg of an antibody specific for mEH (1:1000; Santa Cruz Biotechnology) for 1 h at 4 °C to allow the formation of immune complexes. To precipitate the immune complex, 50 μL of protein G-Sepharose suspension was added to each tube, and the tubes were incubated for 5 h at 4 °C. The immune complexes bound to the Sepharose beads were recovered by centrifugation and washed three times with wash buffer to remove the excess cytosolic fraction. For analysis, the precipitated beads were mixed with SDS-PAGE sample buffer and heated for 10 min at 95 °C. The dissociated proteins were resolved by 10% SDS-PAGE and detected by immunoblotting with an antibody specific for p-PKCδ at Tyr311 (1:500; Santa Cruz Biotechnology) or cleaved-PKCδ (1:1000; Santa Cruz Biotechnology).

2.7. Determination of protein carbonyl

The extent of protein oxidation was assessed by measuring the content of protein carbonyl groups in the striatum, which was determined spectrophotometrically with the 2,4-dinitrophenylhydrazine (DNPH)-labeling procedure (Mai et al., 2019b, 2019c; Nguyen et al., 2018; Shin et al., 2014). The results are expressed as nanomoles of DNPH incorporated/mg protein based on the extinction coefficient for aliphatic hydrazones (21 mM^{-1} cm^{-1}).

2.8. Determination of 4-hydroxynonenal (HNE)

The amount of lipid peroxidation was determined by measuring the level of 4-hydroxynonenal (HNE) using the OxiSelect™ HNE adduct ELISA kit (Cell Biolabs, Inc., San Diego, CA, USA) following the manufacturer's instructions. The striatal homogenate (100 μL) at a protein concentration of 10 μg/mL was incubated in a 96-well protein binding plate at 4 °C overnight. After the protein adsorption, HNE adducts in each well were labeled with HNE antibody followed by incubation with HRP-conjugated secondary antibody. The antibody was detected based on a colorimetric assay using the substrate solution. The absorbance was recorded at 450 nm using a microplate reader (Molecular Devices Inc.). The amount of HNE adduct in each sample was calculated from the standard curve of HNE-BSA (Mai et al., 2019b, 2019c; Nguyen et al., 2018).

2.9. Determination of reactive oxygen species (ROS)

The reactive oxygen species (ROS) formation in the striatum was assessed by measuring the conversion of 2′,7′-dichlorofluorescin diacetate (DCFH-DA) to dichlorofluorescin (DCF) (Mai et al., 2019b, 2019c; Nguyen et al., 2018). The striatal homogenates were added to a tube containing 2 mL of phosphate buffer saline (PBS) with 10 nmol of DCFH-DA, dissolved in methanol. The mixture was incubated at 37 °C for 3 h, and the fluorescence was measured (excitation wavelength of 480 nm and emission wavelength of 525 nm). DCF was used as a standard.

2.10. Immunocytochemistry

Immunocytochemistry was performed as described previously (Dang et al., 2018a; Mai et al., 2019c; Shin et al., 2014). Mice were perfused transcardially with 50 mL of ice-cold PBS (10 mL/10 g body weight) followed by perfusion with 4% paraformaldehyde (20 mL/10 g body weight). The brain was excised and stored in 4% paraformaldehyde overnight. A series of every sixth section (35 μm thickness, 210 μm apart) from the striatum was selected and subjected to immunocytochemistry. The sections were blocked with PBS containing 0.3% hydrogen peroxide for 30 min. The sections were then incubated in PBS containing 0.4% Triton X-100 and 1% normal serum for 20 min. The sections were incubated with a primary antibody against TH (1:500; Chemicon, EMD Millipore) for 48 h, followed by incubation with biotinylated secondary antibody (1:1000; Vector Laboratories, Burlingame, CA, USA) for 1 h. The sections were then immersed in a solution containing avidin-biotin peroxidase complex (Vector Laboratories) for 1 h. We used 3,3′-diaminobenzidine as the chromogen. Digital images were acquired under an upright microscope (BX51; Olympus, Tokyo, Japan) fitted with a digital microscope camera (DP72; Olympus) and an IBM-compatible PC. The immunoreactivity of TH was measured using ImageJ software version 1.47 (National Institutes of Health, Bethesda, MD, USA) as described previously (Dang et al., 2018a; Mai et al., 2019b). Briefly, the images were subjected to background subtraction to correct for uneven background. The entire striatal region (for TH-immunoreactivity) was drawn as the region of interest (ROI). The mean density was measured after selecting the hue, saturation, and brightness threshold values in the “Adjust Color Threshold” dialog box of the immunoreactive area.

2.11. Measurement of dopamine and its metabolites

Mice were sacrificed by cervical dislocation, and the brain was excised. The striatum was dissected out and immediately frozen on dry ice and stored at −70 °C until extraction. The striatum obtained from each animal was weighed and subjected to ultrasonication in 10% perchloric acid containing the internal standard dihydroxybenzylamine (10 ng/mg of the tissue). The lysate was centrifuged at 20000 *g* for 10 min. The level of dopamine and its metabolites, 3,4-dihydroxyphenylacetic acid (DOPAC), and homovanillic acid (HVA) was determined by HPLC coupled with electrochemical detection as described previously (Dang et al., 2018a; Shin et al., 2014). The supernatant (20 μL) was injected into the HPLC equipped with a 3 μm C18 column. The mobile phase was comprised of 26 mL acetonitrile, 21 mL tetrahydrofuran and 960 mL 0.15 M monochloroacetic acid (pH 3.0) containing 50 mg/L EDTA and 200 mg/L sodium octyl sulfate. The amount of dopamine, DOPAC and HVA was determined by comparing the peak area of tissue sample with that of the standard. The amount was expressed as microgram per gram of wet tissue (Dang et al., 2018a, 2018b; Nguyen et al., 2018).

2.12. Locomotor activity

Locomotor activity was measured for 30 min using an automated video-tracking system (Noldus Information Technology, Wagenin, The Netherlands). Four test boxes (40 × 40 × 30 cm high) were operated simultaneously by an IBM computer. Mice were studied individually for the locomotor activity in each test box. The mice were allowed to adapt for 5 min before starting the experiment. A printout for each session showed the pattern of the ambulatory movements of the test box. The distance traveled (in centimeter) by the animals in the horizontal locomotor activity was analyzed. Data were collected and analyzed between 09:00 and 17:00 h (Dang et al., 2017a; Nguyen et al., 2015, 2018; Tran et al., 2018b).

2.13. Rotarod test

Rotarod test was performed 1 h after the locomotor activity measurement. The apparatus (Ugo Basile model 7650, Comerio, VA, Italy) consisted of a base platform and a rotating rod with a non-slippery surface. The rod was placed at a height of 15 cm from the base. The rod (30 cm in length) was divided into 5 equal sections by 6 opaque disks (so that the subjects cannot be distracted by one another). To assess the motor performance, the mice were first trained on the apparatus for 2 min at a constant rotation of 4 rpm. The test was performed 30 min after training and an accelerating paradigm was applied, starting from a rotation speed of 4 rpm up to a maximum speed of 40 rpm. The rotation speed was then kept constant at 40 rpm for a maximum period of 300 s. The duration for which the animal could maintain the balance on the rotating drum was measured as the latency to fall, with a maximal cut-off time of 300 s (Dang et al., 2017a; Nguyen et al., 2018; Shin et al., 2014).

2.14. Statistical analyses

The data were analyzed using IBM SPSS ver. 21.0 (IBM, Chicago, IL, USA). Repeated-measures analysis of variance (ANOVA) was employed to analyze the rectal temperature data. One-way ANOVA or two-way ANOVA was employed for statistical analyses followed by post-hoc test, Fisher's least significant difference pairwise comparison. The data were considered statistically significant when the p value was less than 0.05.

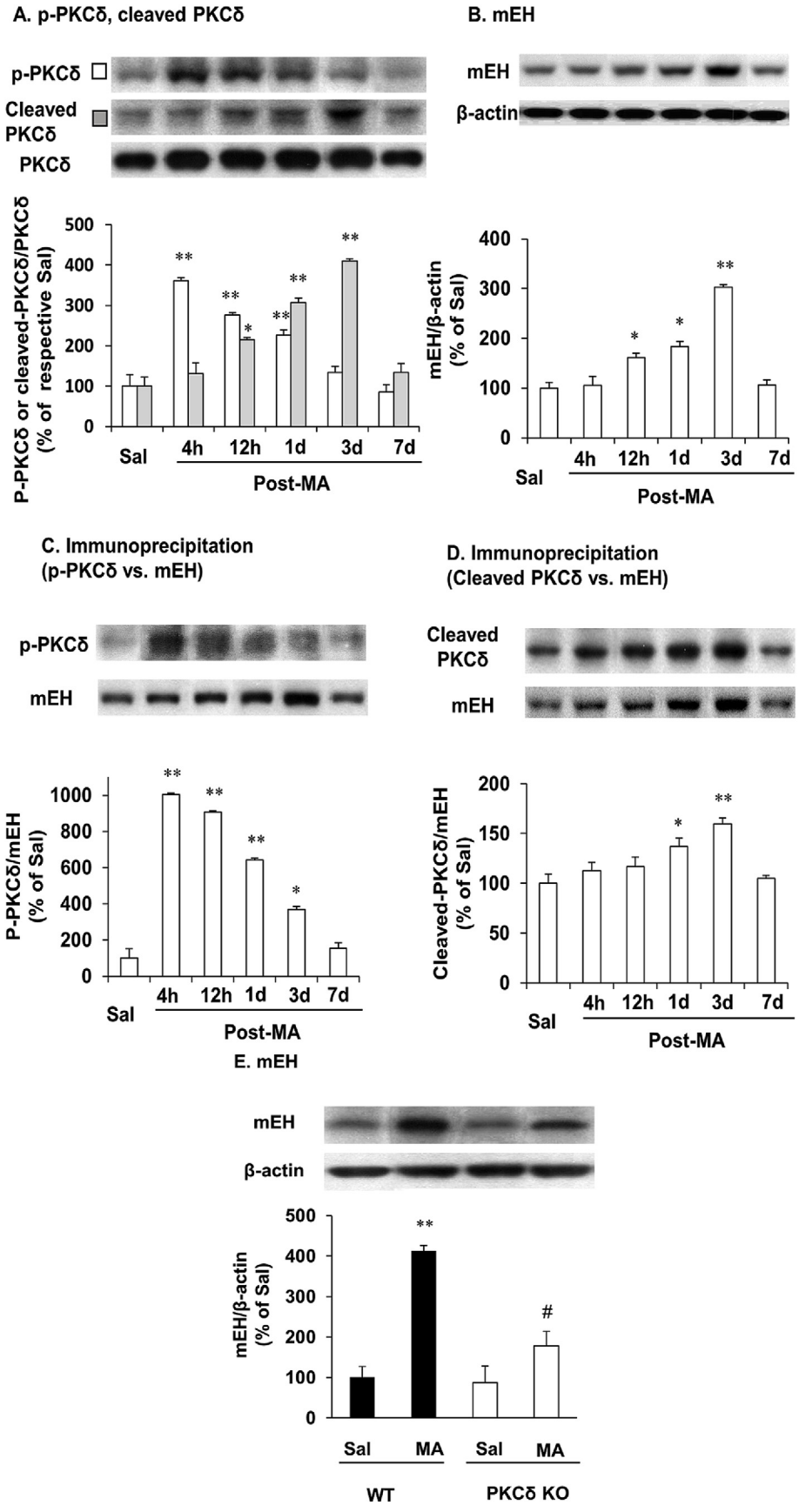

Fig. 2. Time-course of change in phosphorylated protein kinase Cδ (p-PKCδ) and cleaved-PKCδ expression (A), microsomal epoxide hydrolase (mEH) expression (B), interaction between p-PKCδ and mEH (C), and interaction between cleaved-PKCδ and mEH (D) in the striatum of WT mice after the final methamphetamine (MA) treatment, and the effect of gene knockout of PKCδ on MA-induced mEH expression (E) in mice. Sal = saline. WT = wild-type mice. Data are represented as the mean ± SEM of six mice. $^{*}p < 0.05$, $^{**}p < 0.01$ vs. corresponding saline, $^{\#}p < 0.01$ vs. corresponding MA/WT (A-D; one-way ANOVA, and E; two-way ANOVA for repeated measures followed by Fisher's LSD pairwise comparison).

3. Results

3.1. MA induces enhanced interaction between p-PKCδ/cleaved-PKCδ and mEH and effect of genetic inhibition of PKCδ on MA-induced mEH expression in mice

We examined the time-course of MA-induced change in the striatal expression of p-PKCδ, cleaved-PKCδ, and mEH (Fig. 1). We observed a significant increase in p-PKCδ expression at 4 h ($p < 0.01$ *vs.* saline treatment), 12 h ($p < 0.01$ *vs.* saline treatment), and day 1 ($p < 0.01$ *vs.* saline treatment) post-MA treatment. The enhanced expression appeared to be prominent at 4 h post-MA treatment. The expression of cleaved-PKCδ was significantly enhanced at 12 h ($p < 0.05$ *vs.* saline treatment), day 1 ($p < 0.01$ *vs.* saline treatment), and day 3 ($p < 0.01$ *vs.* saline treatment) post-MA treatment. The enhanced expression was most prominent at day 3 post-MA treatment (Fig. 2A). Additionally, the enhanced expression of mEH was observed at 12 h ($p < 0.05$ *vs.* saline treatment), day 1 ($p < 0.05$ *vs.* saline treatment), and day 3 ($p < 0.01$ *vs.* saline treatment) post-MA treatment (Fig. 2B). The enhanced expression of mEH induced by MA appeared to be maximal at day 3 post-MA treatment. We used immunoprecipitation to investigate the interaction between p-PKCδ/cleaved-PKCδ and mEH. We observed a significant increase in the interaction between p-PKCδ and mEH at 4 h ($p < 0.01$ *vs.* saline treatment), 12 h ($p < 0.01$ *vs.* saline treatment), day 1 ($p < 0.01$ *vs.* saline treatment), and day 3 ($p < 0.05$ *vs.* saline treatment) post-MA treatment (Fig. 2C). The maximal interaction was observed at 4 h post-MA treatment. In contrast, the interaction between cleaved-PKCδ and mEH significantly increased at day 1 ($p < 0.05$ *vs.* saline treatment), and day 3 ($p < 0.01$ *vs.* saline treatment) post-MA treatment. The maximal interaction was observed at day 3 post-MA treatment (Fig. 2D). As shown in Fig. 2E, PKCδ knockout mice exhibited significant attenuation of the enhanced expression of mEH induced by MA ($p < 0.01$ *vs.* MA/WT). Consistently, PKCδ and mEH immunoreactivity was co-localized in the same cell (Supplementary Fig. S2).

3.2. Effect of gene knockout of PKCδ and mEH on the hyperthermia induced by MA in mice

Earlier studies have suggested that hyperthermia may be important for the MA-induced dopaminergic neurotoxicity (Riddle et al., 2006; Shin et al., 2011, 2018b). We examined whether gene knockout of PKCδ or mEH affects the MA-induced hyperthermia in mice. As shown in Fig. 3, MA treatment significantly induced hyperthermia ($p < 0.01$ *vs.* saline treatment) in the WT mice. Further, PKCδ or mEH knockout mice exhibited significant attenuation of the MA-induced hyperthermia

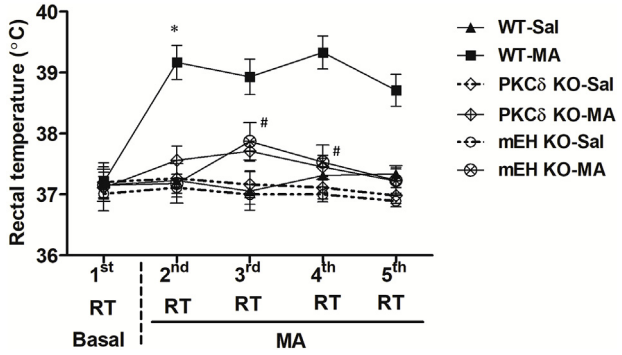

Fig. 3. Effect of gene knockout of protein kinase Cδ (PKCδ) and microsomal epoxide hydrolase (mEH) on methamphetamine (MA)-induced hyperthermia in mice. Sal = saline. WT = wild-type mice. Data are represented as the mean ± S.E.M of six mice. *$p < 0.01$ vs. corresponding saline, #$p < 0.01$ vs. corresponding MA/WT (two-way ANOVA for repeated measures followed by Fisher's LSD pairwise comparison).

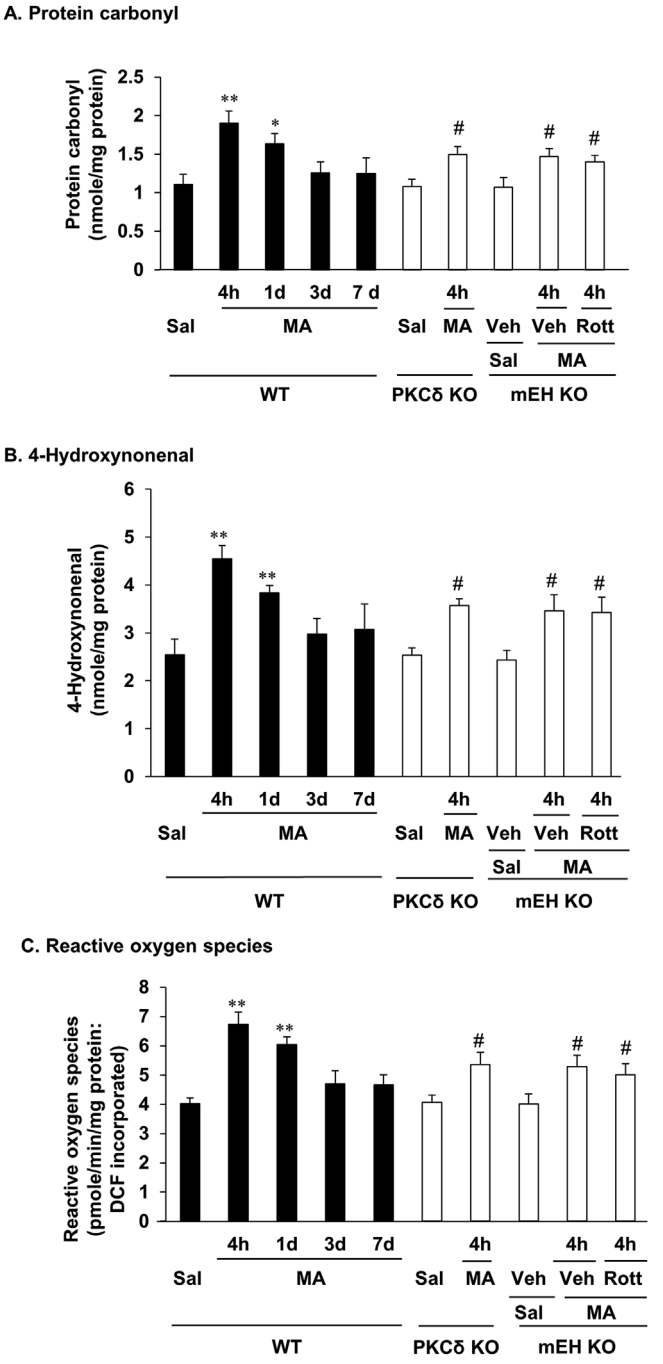

Fig. 4. Time-course of change in protein carbonyl group (A), 4-hydroxynonenal (HNE) (B), and reactive oxygen species (ROS) (C) induced by MA in the striatum of WT mice, and the effects of protein kinase Cδ (PKCδ) gene knockout and microsomal epoxide hydrolase (mEH) gene knockout with PKCδ inhibition on protein carbonyl, HNE and ROS levels induced by MA in mice (A–C). Sal = saline. WT = wild-type mice. Veh = vehicle [10% (v/v) DMSO]. Data are represented as the mean ± S.E.M of six mice. *$p < 0.05$, **$p < 0.01$ vs. corresponding saline, #$p < 0.05$ vs. corresponding MA/WT (one-way ANOVA followed by Fisher's LSD pairwise comparison).

(MA/WT *vs.* MA/PKCδ KO; $p < 0.01$ or MA/WT *vs.* MA/mEH KO; $p < 0.01$).

3.3. PKCδ knockout mice and mEH knockout mice exhibit attenuation of enhanced oxidative stress induced by MA treatment

We investigated the effect of PKCδ inhibition on the MA-induced

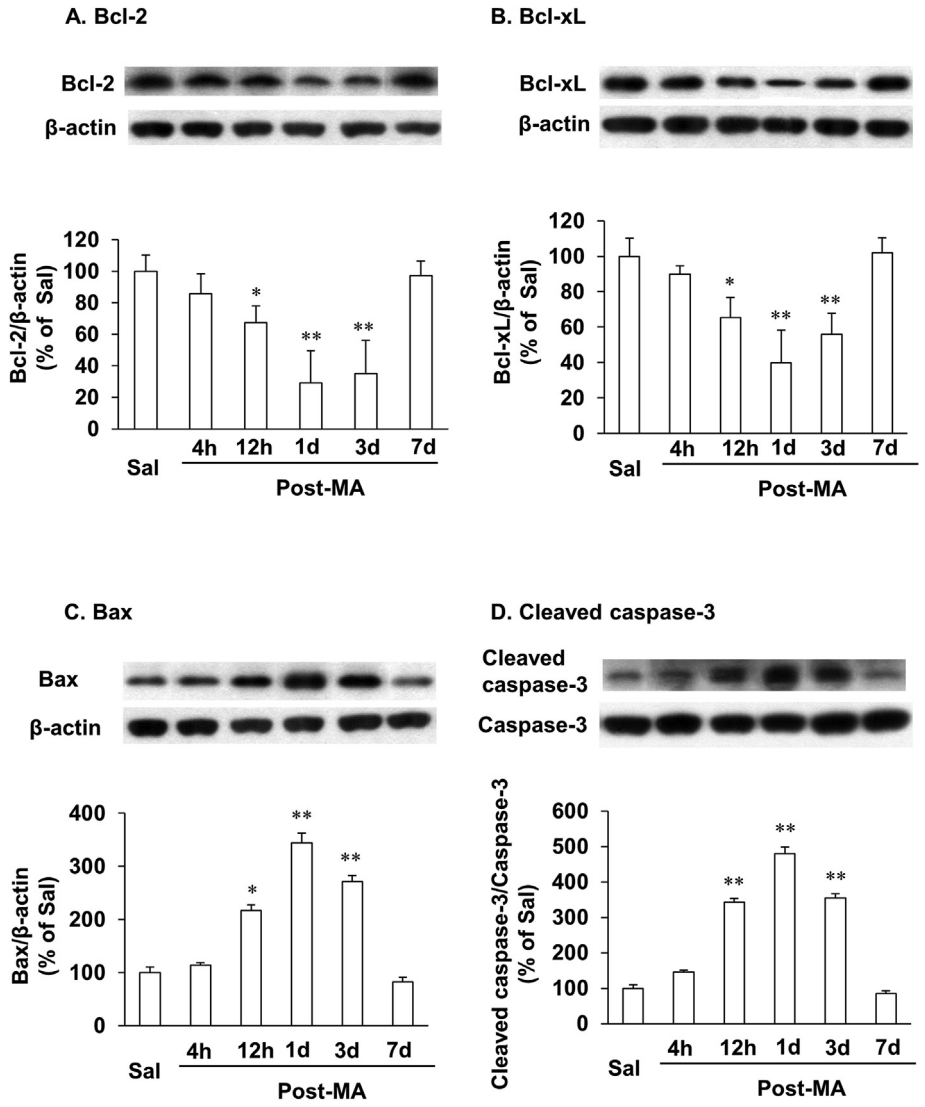

Fig. 5. Time-course of change in the expression of Bcl-2 (A), Bcl-xl (B), Bax (C), and cleaved caspase-3 (D) induced by methamphetamine (MA) in the striatum of WT mice, and the effect of protein kinase Cδ (PKCδ) gene knockout and microsomal epoxide hydrolase (mEH) gene knockout with PKCδ inhibition on the expression of Bcl-2 (E), Bcl-xl (F), Bax (G), Bax/Bcl-2 ratio (H) and cleaved caspase-3 (I) induced by MA in mice. Sal = saline. WT = wild-type mice. Veh = vehicle [10% (v/v) DMSO]. Data are represented as the mean ± SEM of six mice. $^{*}p < 0.05$, $^{**}p < 0.01$ vs. corresponding saline, $^{\#}p < 0.01$ vs. corresponding MA/WT (one-way ANOVA followed by Fisher's LSD pairwise comparison).

oxidative stress in mEH knockout mice by measuring the levels of protein carbonyl group, HNE, and ROS (Fig. 4A–C). We observed significantly enhanced levels of protein carbonyl group, HNE, and ROS in the striatum of WT mice (protein carbonyl group, $p < 0.01$ *vs.* saline treatment; HNE, $p < 0.01$ *vs.* saline treatment; ROS, $p < 0.01$ *vs.* saline treatment) at 4 h post-MA treatment. The elevated levels of protein carbonyl group, HNE, and ROS persisted even at day 1 post-MA treatment (protein carbonyl group, $p < 0.05$ *vs.* saline treatment; HNE, $p < 0.01$ *vs.* saline treatment; ROS, $p < 0.01$ *vs.* saline treatment) in the WT mice. However, their levels returned to near control (saline) levels at day 3 post-MA treatment. PKCδ knockout mice exhibited significant attenuation of enhanced oxidative stress (as measured by enhanced levels of protein carbonyl group, HNE, and ROS) at 4 h (protein carbonyl group, HNE or ROS; $p < 0.05$ *vs.* MA/WT) post-MA treatment. Importantly, the attenuation of enhanced oxidative stress observed in the mEH knockout mice was comparable to that observed in the PKCδ knockout mice. However, when the mEH knockout mice were treated with rottlerin, it did not result in any additive beneficial effect against oxidative stress. Consistently, both PKCδ knockout and mEH knockout mice exhibited significant attenuation of the elevated levels of protein carbonyl group, HNE, and ROS at day 1 post-MA treatment (Supplementary Fig. S2).

3.4. The effects of PKCδ knockout and mEH knockout with PKCδ inhibitor rottlerin on the proapoptotic potential induced by MA in mice

As shown in Fig. 5A–D, we examined time-course of changes in the levels of Bcl-2, Bcl-xl, Bax, and cleaved caspase-3 after the final MA treatment. MA treatment decreased the expression of anti-apoptotic proteins Bcl-2 (12 h, $p < 0.05$ *vs.* saline; 1 d, $p < 0.01$ *vs.* saline; 3 d, $p < 0.01$ *vs.* saline) (Fig. 5A), and Bcl-xl (12 h, $p < 0.05$ *vs.* saline; 1 d, $p < 0.01$ *vs.* saline; 3 d, $p < 0.01$ *vs.* saline) (Fig. 5B) in WT mice. In contrast, MA treatment increased the levels of the pro-apoptotic factors Bax (12 h, $p < 0.05$ *vs.* saline; 1 d, $p < 0.01$ *vs.* saline; 3 d, $p < 0.01$ *vs.* saline) (Fig. 5C), and cleaved-caspase-3 (12 h, $p < 0.01$ *vs.* saline; 1 d, $p < 0.01$ *vs.* saline; 3 d, $p < 0.01$ *vs.* saline) (Fig. 5D) in the WT mice. All the anti/pro-apoptotic factors returned to near control (saline) level 7 d later. Because MA-induced anti-apoptotic and pro-apoptotic changes were most evident 1 d post-MA, we examined the effects of PKCδ knockout and mEH knockout 1 d post-MA in mice. As shown in

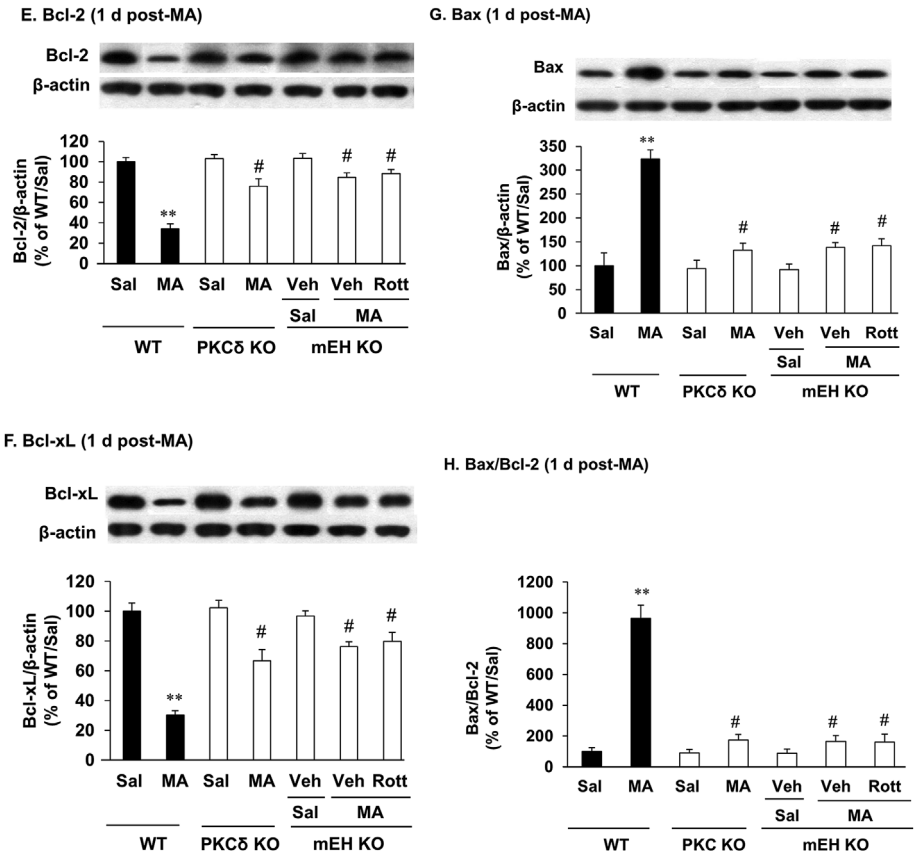

Fig. 5. (*continued*)

Fig. 5E–H, PKCδ knockout significantly attenuated MA-induced changes in Bcl-2 ($p < 0.01$ *vs.* MA/WT), Bcl-xl ($p < 0.01$ *vs.* MA/WT), Bax ($p < 0.01$ *vs.* MA/WT), and cleaved-caspase-3 ($p < 0.01$ *vs.* MA/WT).

We examined the time-course of MA-induced change in the levels of Bcl-2, Bcl-xl, Bax, and cleaved caspase-3 (Fig. 5A–D). Treatment with MA significantly decreased the expression of anti-apoptotic proteins, Bcl-2 (12 h, $p < 0.05$ *vs.* saline treatment; day 1, $p < 0.01$ *vs.* saline treatment; day 3, $p < 0.01$ *vs.* saline treatment) (Fig. 5A), and Bcl-xl (12 h, $p < 0.05$ *vs.* saline treatment; day 1, $p < 0.01$ *vs.* saline treatment; day 3, $p < 0.01$ *vs.* saline treatment) (Fig. 5B) in the WT mice. Contrastingly, treatment with MA significantly increased the expression of the pro-apoptotic proteins Bax (12 h, $p < 0.05$ *vs.* saline; 1 d, $p < 0.01$ *vs.* saline; 3 d, $p < 0.01$ *vs.* saline) (Fig. 5C), and cleaved-caspase-3 (12 h, $p < 0.01$ *vs.* saline; 1 d, $p < 0.01$ *vs.* saline; 3 d, $p < 0.01$ *vs.* saline) (Fig. 5D) in the WT mice. The expression level of all anti/pro-apoptotic factors returned to near control (saline) levels at day 7 post-MA treatment. As the MA-induced change in the expression anti-apoptotic and pro-apoptotic genes was most evident at day 1 post-MA, we examined the effect of PKCδ gene knockout and mEH gene knockout in mice at this time point. As shown in Fig. 5E–I, the PKCδ knockout mice exhibited significant attenuation of the MA-induced changes in the expression of Bcl-2 ($p < 0.01$ *vs.* MA/WT), Bcl-xl ($p < 0.01$ *vs.* MA/WT), Bax ($p < 0.01$ *vs.* MA/WT), Bax/Bcl-2 ratio ($p < 0.01$ *vs.* MA/WT) and cleaved-caspase-3 ($p < 0.01$ *vs.* MA/WT). The anti-apoptotic potential by PKCδ knockout is clearly comparable to that by mEH knockout. When the mEH knockout mice were treated with rottlerin we did not observe any additive effect on the expression of apoptotic proteins (Fig. 5E–H).

3.5. PKCδ knockout and mEH knockout mice exhibit attenuation of dopaminergic defects

We examined the time-course of MA-induced changes in TH expression, dopamine level, and dopamine turnover rate (Fig. 6A–C). There was a significant decrease in the expression of TH at day 1 ($p < 0.05$ *vs.* saline treatment), day 3 ($p < 0.01$ *vs.* saline treatment), and day 7 ($p < 0.05$ *vs.* saline treatment) post-MA treatment (Fig. 6A). Further, we observed a significant decrease in the dopamine level at 12 h ($p < 0.05$ *vs.* saline treatment), day 1 ($p < 0.01$ *vs.* saline treatment), day 3 ($p < 0.01$ *vs.* saline treatment), and day 7 ($p < 0.01$ *vs.* saline treatment) post-MA treatment (Fig. 6B). In contrast, the dopamine turnover rate was significantly enhanced at 12 h ($p < 0.05$ *vs.* saline treatment), day 1 ($p < 0.05$ *vs.* saline treatment), day 3 ($p < 0.01$ *vs.* saline treatment), and day 7 ($p < 0.05$ *vs.* saline treatment) post-MA treatment (Fig. 6C). As these MA-induced dopaminergic impairments were prominent at day 3 post-MA treatment, we focused on this time-point for further analysis. PKCδ knockout and mEH knockout mice exhibited significant attenuation of the MA-induced change in TH expression/TH immunoreactivity (MA/WT *vs.* MA/PKCδ KO; $p < 0.01$ or MA/WT *vs.* MA/mEH KO; $p < 0.01$) (Fig. 6D and E), dopamine level (MA/WT *vs.* MA/PKCδ KO; $p < 0.01$ or MA/WT *vs.* MA/mEH KO; $p < 0.01$) (Fig. 6F), and dopamine turnover rate (MA/WT *vs.* MA/PKCδ KO; $p < 0.01$ or MA/WT *vs.* MA/mEH KO; $p < 0.01$) (Fig. 6G). When mEH knockout mice were treated with rottlerin, it did not result in any additive beneficial effect on the dopaminergic changes.

3.6. PKCδ knockout and mEH knockout mice exhibit attenuation of the behavioral defects induced by MA treatment

As MA-induced behavioral defects (i.e., locomotor activity and rotarod performance) might be related to the dopaminergic impairment, we examined whether gene knockout of mEH and PKCδ could attenuate the behavioral defects induced by MA in mice. We examined the time-course of MA-induced impairment in locomotor activity and rotarod performance (Fig. 7A and B). We observed a significant decrease in the locomotor activity at day 1 ($p < 0.05$ *vs.* saline treatment), day 3

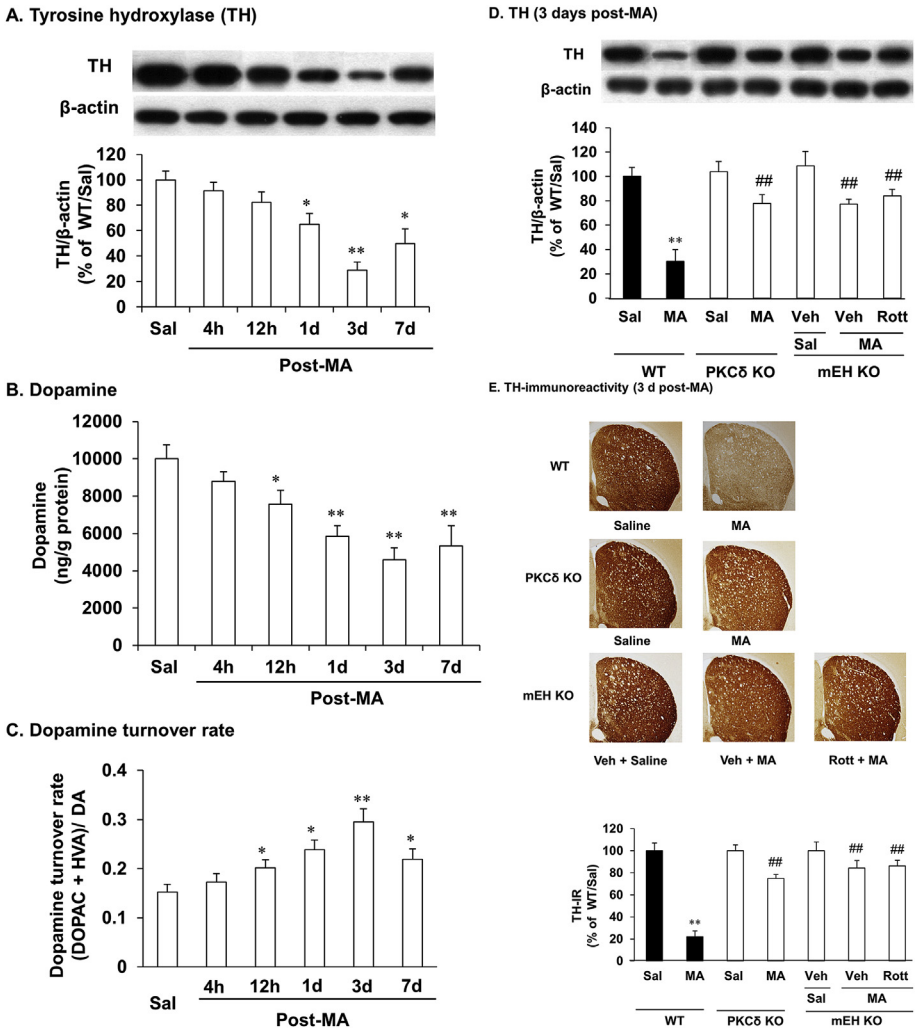

Fig. 6. Time-course of change in tyrosine hydroxylase (TH) expression (A), dopamine (DA) level (B), and DA turnover rate (C) induced by methamphetamine (MA) in the striatum of WT mice, and effect of protein kinase Cδ (PKCδ) gene knockout and microsomal epoxide hydrolase (mEH) gene knockout with PKCδ inhibition on TH expression (D), TH-immunoreactivity (E), DA level, (F) and DA turnover rate (G) induced by MA in mice. Sal = saline. WT = wild-type mice. Veh = vehicle [10% (v/v) DMSO]. Data are represented as the mean ± SEM of six mice. $^{*}p < 0.05$, $^{**}p < 0.01$ vs. corresponding saline, $^{\#}p < 0.05$, $^{\#\#}p < 0.01$ vs. corresponding MA/WT (one-way ANOVA followed by Fisher's LSD pairwise comparison).

($p < 0.01$ *vs.* saline treatment), and day 7 ($p < 0.05$ *vs.* saline treatment) post-MA treatment (Fig. 7A). The locomotor activity of mice was consistently similar to their rotarod performance (Fig. 7B). As shown in Fig. 7C and D, PKCδ knockout and mEH knockout mice exhibited significant attenuation of hypolocomotion (MA/WT *vs.* MA/PKCδ KO; $p < 0.01$ or MA/WT *vs.* MA/mEH KO; $p < 0.01$), and impaired rotarod performance (MA/WT *vs.* MA/PKCδ KO; $p < 0.01$ or MA/WT *vs.* MA/mEH KO; $p < 0.01$) induced by MA. When mEH knockout mice were treated with rottlerin, it did not have any additive beneficial effect on the behavioral defect. Consistently, PKCδ knockout and mEH knockout mice exhibited significant attenuation of impaired locomotor activity and rotarod performance at day 7 post-MA treatment (Supplementary Fig. S3).

4. Discussion

Previously, we had described the significance of PKCδ in MA-induced dopaminergic neurotoxicity (Dang et al., 2015, 2018b; Nguyen et al., 2015; Shin et al., 2011, 2012, 2019). We reported that MA treatment results in early phosphorylation of PKCδ in the striatum of mice (Dang et al., 2018b). Further, it was also demonstrated that H_2O_2-mediated phosphorylation of PKCδ at Tyr311 is implicated in the regulation of caspase-3-mediated proteolytic cleavage of PKCδ and its proapoptotic function during dopaminergic neuronal cell death (Kaul et al., 2005). PKCδ, a stress sensitive kinase, is identified as an effector molecule of dopaminergic cell death in MA-induced neurodegeneration (Dang et al., 2016; Nguyen et al., 2015; Shin et al., 2011, 2012, 2014, 2018a, 2018b, 2019).

In this study, we demonstrated for the first time that p-PKCδ co-immunoprecipitated with mEH (maximum; 4 h post-MA treatment) and that the cleaved-PKCδ co-immunoprecipitated with mEH (maximum; day 3 post-MA treatment). PKCδ knockout in mice resulted in attenuation of mEH induction post-MA treatment. Similarly, mEH knockout resulted in the attenuation of dopaminergic impairment and behavioral defect induced by MA treatment. Importantly, the PKCδ inhibitor, rottlerin, had no further effect on the dopaminergic changes observed in the mEH knockout mice, indicating that mEH gene is a critical mediator for PKCδ-induced dopaminergic toxicity. Therefore, it is plausible that mEH may be a downstream target for PKCδ-mediated dopaminergic neurotoxicity induced by MA (Fig. 8).

It was previously reported that the pharmacological inhibition of PKC suppresses the expression of xenobiotic-metabolizing/detoxifying enzymes, including mEH and certain CYP450 isoforms (Kim et al., 1998). We demonstrated that the expression of mEH was suppressed in the PKCδ knockout mice. We previously demonstrated that treatment with trimethyltin, an environmental neurotoxin, resulted in enhanced mEH expression in the rat brain (Liu et al., 2006). This concurred with the results of the current study where MA treatment resulted in enhanced mEH expression. It is known that the induction of mEH expression is always associated with the enhanced expression of CYP450 isoforms. mEH is a critical biotransformation enzyme that catalyzes the *trans*-addition of water to the highly reactive intermediary metabolites (i.e., epoxides), formed during CYP450-dependent oxidation of unsaturated aliphatic and aromatic xenobiotics, to convert them into less

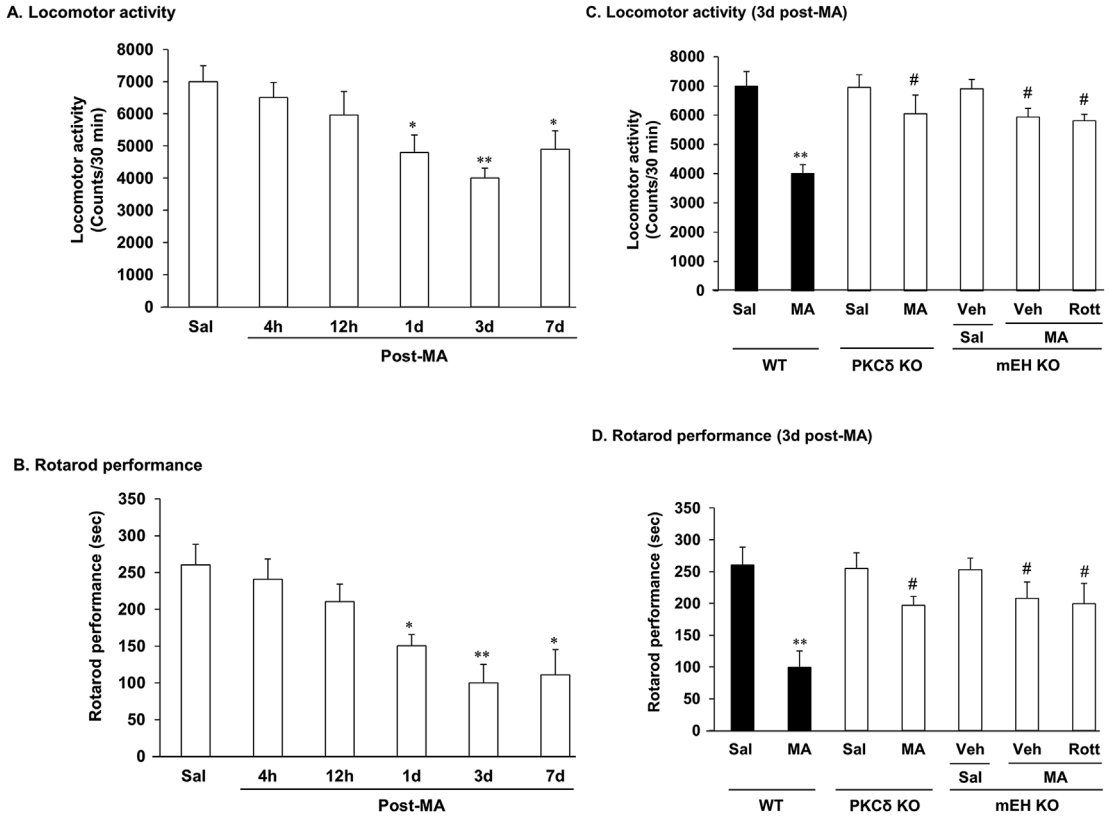

Fig. 7. Time-course of change in locomotor activity (A), and rotarod performance (B) induced by methamphetamine (MA) in mice, and the effect of protein kinase Cδ (PKCδ) gene knockout and microsomal epoxide hydrolase (mEH) gene knockout with PKCδ inhibition on locomotor activity (C) and rotarod performance (E) induced by MA in mice. Sal = saline. WT = wild-type mice. Veh = vehicle [10% (v/v) DMSO]. Data are represented as the mean ± SEM of six mice. $^{*}p < 0.05$, $^{**}p < 0.01$ vs. corresponding saline, $^{\#}p < 0.01$ vs. corresponding MA/WT (one-way ANOVA followed by Fisher's LSD pairwise comparison).

reactive intermediates (Fretland and Omiecinski, 2000; Srivastava, 2016). It is plausible that these intermediates might further metabolize into *ortho*-quinone that can enter into a redox cycle using NADPH to induce oxidative stress (Bolton et al., 2000; Park et al., 2005). Oxidative stress induces PKC signaling pathway, which plays an important role in the induction of CYP450 isozyme (Jin et al., 2012). Indeed, it has been suggested that CYP450 isozyme participates in the oxidative metabolism of MA for generating potent neurotoxic metabolites (Cherner et al., 2010).

Previously, we had reported that mEH gene acts as an endogenous modulator in response to MA drug dependence. We demonstrated that the mEH protein is localized to astrocytes, and the astrocytic mobilization of mEH might play an important role in attenuating the MA drug dependence (Shin et al., 2009). We also demonstrated that mEH immunoreactivity is expressed in reactive astrocytes after treatment with trimethyltin (Liu et al., 2006), or 1-methyl-4-phenyl-1,2,3,6-tetrahydropyridine (MPTP) (Liu et al., 2008). Therefore, it is possible that astrocytic modulation is also important for both neuroprotective and neurotoxic mechanisms. However, the dual role of mEH in neurotoxic and neuroprotective conditions has to be further elucidated.

Earlier studies reported that the enhanced expression of mEH is associated with the enhanced expression of the proapoptotic protein, Bax (Shahid et al., 2016; Springer et al., 1996). Previously, we (Dang et al., 2017b; Nguyen et al., 2015), and others (Jayanthi et al., 2001) have reported that MA treatment up-regulates the expression of pro-apoptotic protein (Bax) and down-regulates the anti-apoptotic proteins (Bcl-2, Bcl-xl) in the brain, which consequently induce cell death *via* PKCδ-dependent pathway. Therefore, early interaction between p-PKCδ and mEH and late interaction between cleaved-PKCδ and mEH might be the critical signaling process for MA-induced cell death mechanism.

Hyperthermia might facilitate intracellular accumulation of MA (Xie et al., 2000). As the attenuation of hyperthermia can be protective against MA-induced neurotoxicity (Riddle et al., 2006), it is plausible that hyperthermia might mediate MA-induced oxidative stress initially (Shin et al., 2011). Thus, it is possible that the thermoregulation observed in PKCδ knockout and mEH knockout mice contributes to the attenuation of oxidative stress.

It has been suggested that mEH forms a complex with CYP450 in the endoplasmic reticulum (Orjuela Leon et al., 2017). Importantly, it has also been shown that CYP450 is a substrate for PKC (Vilgrain et al., 1984), and that CYP450 phosphorylation by PKC results in enhanced CYP450 enzymatic activity (Aguiar et al., 2005). However, the role of CYP450 in modulating the interaction between p-PKCδ/cleaved-PKCδ and mEH is yet to be elucidated.

MA-induced dopamine release might be responsible for the oxidative stress, mitochondrial dysfunction and pro-apoptotic changes (i.e. activation of caspases and increases in Bax expression) (Krasnova et al., 2009; Dang et al., 2017b; Thrash-Williams et al., 2016). In our recent study, we demonstrated that MA causes pro-apoptotic changes in the dopaminergic terminal possibly via upregulation of dopamine D2 receptor (D2R) and CB1R in the striatum (Dang et al., 2017a). In addition, MA facilitated dopamine-dependent caspase activation in cultured striatal cell line with Bax expression (Deng et al., 2002).

We demonstrated that mEH mediates MPTP-induced dopaminergic toxicity via inhibiting phosphorylation of TH at Ser^{31} residue (Liu et al., 2008) and that MA-induced PKCδ impairs dopaminergic system via inhibition of phosphorylation of TH at Ser^{40} residue in the striatum (Shin et al., 2011). Moreover, it was reported that MPTP treatment activates PKCδ signaling followed by dopaminergic degeneration (Zhang et al., 2007a). Thus, previous findings (Liu et al., 2008; Shin et al., 2011; Zhang et al., 2007b) may be in line with current finding. Although the role of interaction between PKCδ and mEH in MA-induced

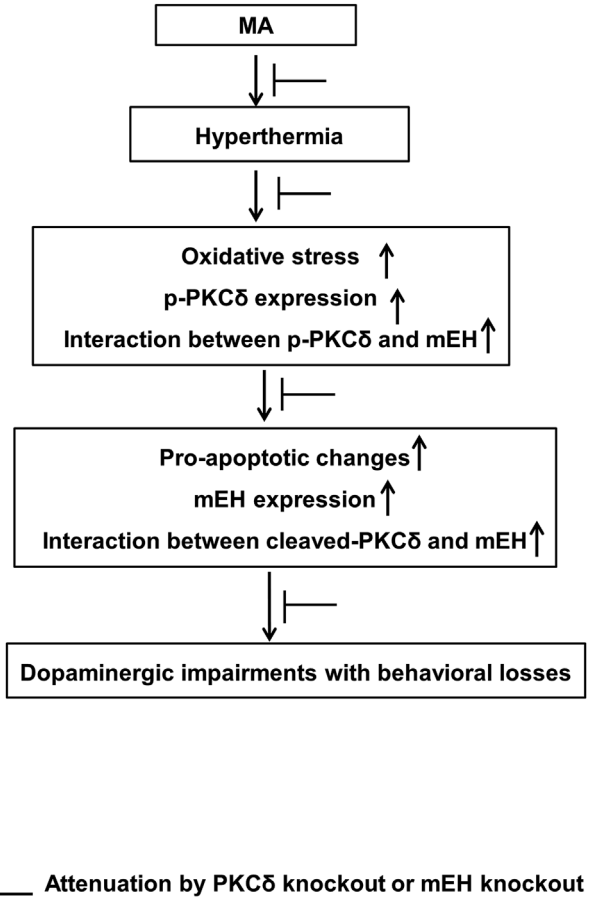

Fig. 8. A schematic depiction of the modulation of protein kinase Cδ (PKCδ) and microsomal epoxide hydrolase (mEH) interaction in methamphetamine (MA)-induced dopaminergic neurotoxicity. Treatment with MA (8 mg/kg, i.p. 4 doses at 2 h interval) resulted in hyperthermia, followed by initial oxidative stress, phosphorylation of PKCδ (p-PKCδ) and interaction between p-PKCδ and mEH. These changes lead to significant increase in mEH expression, cleaved-PKCδ expression, interaction between cleaved-PKCδ and mEH, and pro-apoptotic gene expression. These signaling processes contribute to the dopaminergic and behavioral impairments. These signaling pathways are attenuated by PKCδ gene knockout or mEH gene knockout. Treating mEH mice with the PKCδ inhibitor, rottlerin did not result in any additional effect on the dopaminergic changes. Therefore, we suggest that mEH is a critical mediator for PKCδ-induced dopaminergic neurotoxicity induced by MA.

dopaminergic toxicity remains to be further determined, two genes might be critical components for the pathogenesis on the dopaminergic degeneration. In addition, the significance of PKCδ as an upstream molecule on the mEH induction remains to be characterized. Unexpectedly, we observed here that MA induces a very low mEH-immunoreactivity in the striatum, and that all the mEH-immunoreactivity is presented in PKCδ positive cells in the striatum. It remains to be further elucidated how and why this phenomenon can be occurred.

In summary, we propose that mEH is a downstream molecule in PKCδ-mediated dopaminergic neurotoxicity induced by MA. We suggest that the early induction of p-PKCδ triggers the expression of cleaved-PKCδ and mEH, which is accompanied by neurotoxic pro-apoptotic signals. We also suggest that the interaction between PKCδ and mEH is integral to MA-induced dopaminergic toxicity. The elucidation of this interaction might provide a clue for the therapeutic intervention in MA intoxication.

Declaration of interests

The authors declare that they have no known competing financial interests or personal relationships that could have appeared to influence the work reported in this paper.Acknowledgment

This study was supported by Basic Science Research Program through the National Research Foundation of Korea funded by the Ministry of Science and ICT (#NRF-2019R1I1A3A01063609 and #NRF-2019R1A2C4070161), Republic of Korea. Garima Sharma, Naveen Sharma, Duc Toan Pham, and Quynh Dieu Trinh were supported by the BK21 PLUS program. The English in this document has been checked by at least two professional editors, both native speakers of English (https://app.editage.co.kr/orders/download-files/CAUNE_4715).

Conflicts of interest

The authors have no conflicts of interest to declare.

Appendix A. Supplementary data

Supplementary data to this article can be found online at https://doi.org/10.1016/j.fct.2019.110761.

Transparency document

Transparency document related to this article can be found online at https://doi.org/10.1016/j.fct.2019.110761.

References

Aguiar, M., Masse, R., Gibbs, B.F., 2005. Regulation of cytochrome P450 by post-translational modification. Drug Metab. Rev. 37, 379–404.
Beauvais, G., Atwell, K., Jayanthi, S., Ladenheim, B., Cadet, J.L., 2011. Involvement of dopamine receptors in binge methamphetamine-induced activation of endoplasmic reticulum and mitochondrial stress pathways. PLoS One 6, e28946.
Bolton, J.L., Trush, M.A., Penning, T.M., Dryhurst, G., Monks, T.J., 2000. Role of quinones in toxicology. Chem. Res. Toxicol. 13, 135–160.
Cherner, M., Bousman, C., Everall, I., Barron, D., Letendre, S., Vaida, F., Atkinson, J.H., Heaton, R., Grant, I., Group, H., 2010. Cytochrome P450-2D6 extensive metabolizers are more vulnerable to methamphetamine-associated neurocognitive impairment: preliminary findings. J. Int. Neuropsychol. Soc. 16, 890–901.
Dang, D.K., Duong, C.X., Nam, Y., Shin, E.J., Lim, Y.K., Jeong, J.H., Jang, C.G., Nah, S.Y., Nabeshima, T., Kim, H.C., 2015. Inhibition of protein kinase (PK) Cδ attenuates methamphetamine-induced dopaminergic toxicity via upregulation of phosphorylation of tyrosine hydroxylase at Ser40 by modulation of protein phosphatase 2A and PKA. Clin. Exp. Pharmacol. Physiol. 42, 192–201.
Dang, D.K., Shin, E.J., Nam, Y., Ryoo, S., Jeong, J.H., Jang, C.G., Nabeshima, T., Hong, J.S., Kim, H.C., 2016. Apocynin prevents mitochondrial burdens, microglial activation, and pro-apoptosis induced by a toxic dose of methamphetamine in the striatum of mice via inhibition of p47phox activation by ERK. J. Neuroinflammation 13, 12–34.
Dang, D.K., Shin, E.J., Mai, A.T., Jang, C.G., Nah, S.Y., Jeong, J.H., Ledent, C., Yamamoto, T., Nabeshima, T., Onaivi, E.S., Kim, H.C., 2017a. Genetic or pharmacological depletion of cannabinoid CB1 receptor protects against dopaminergic neurotoxicity induced by methamphetamine in mice. Free Radic. Biol. Med. 108, 204–224.
Dang, D.K., Shin, E.J., Tran, H.Q., Kim, D.J., Jeong, J.H., Jang, C.G., Nah, S.Y., Sato, H., Nabeshima, T., Yoneda, Y., Kim, H.C., 2017b. The role of system Xc(-) in methamphetamine-induced dopaminergic neurotoxicity in mice. Neurochem. Int. 108, 254–265.
Dang, D.K., Shin, E.J., Kim, D.J., Tran, H.Q., Jeong, J.H., Jang, C.G., Nah, S.Y., Jeong, J.H., Byun, J.K., Ko, S.K., Bing, G., Hong, J.S., Kim, H.C., 2018a. Ginsenoside Re protects methamphetamine-induced dopaminergic neurotoxicity in mice via upregulation of dynorphin-mediated kappa-opioid receptor and downregulation of substance P-mediated neurokinin 1 receptor. J. Neuroinflammation 15, 52–74.
Dang, D.K., Shin, E.J., Kim, D.J., Tran, H.Q., Jeong, J.H., Jang, C.G., Ottersen, O.P., Nah, S.Y., Hong, J.S., Nabeshima, T., Kim, H.C., 2018b. PKCδ-dependent p47phox activation mediates methamphetamine-induced dopaminergic neurotoxicity. Free Radic. Biol. Med. 115, 318–337.
Deng, X., Cai, N.S., McCoy, M.T., Chen, W., Trush, M.A., Cadet, J.L., 2002. Methamphetamine induces apoptosis in an immortalized rat striatal cell line by activating the mitochondrial cell death pathway. Neuropharmacology 42, 837–845.
Ebihara, S., Marks, T., Hudson, D.J., Menaker, M., 1986. Genetic control of melatonin synthesis in the pineal gland of the mouse. Science 231, 491–493.
Fretland, A.J., Omiecinski, C.J., 2000. Epoxide hydrolases: biochemistry and molecular biology. Chem. Biol. Interact. 129, 41–59.
Giorgi, C., Agnoletto, C., Baldini, C., Bononi, A., Bonora, M., Marchi, S., Missiroli, S.,

Patergnani, S., Poletti, F., Rimessi, A., Zavan, B., Pinton, P., 2010. Redox control of protein kinase C: cell- and disease-specific aspects. Antioxidants Redox Signal. 13, 1051–1085.
Goto, M., Oshima, I., Hasegawa, M., Ebihara, S., 1994. The locus controlling pineal serotonin N-acetyltransferase activity (Nat-2) is located on mouse chromosome 11. Brain Res. Mol. Brain Res. 21, 349–354.
Haavik, J., Schelling, D.L., Campbell, D.G., Andersson, K.K., Flatmark, T., Cohen, P., 1989. Identification of protein phophatase 2A as the major tyrosine hydroxylase phosphatase in adrenal medulla and corpus striatum:evidence from effects of okadaic acid. FEBBS Lett. 17, 36–42.
Jayanthi, S., Deng, X., Bordelon, M., McCoy, M.T., Cadet, J.L., 2001. Methamphetamine causes differential regulation of pro-death and anti-death Bcl-2 genes in the mouse neocortex. FASEB J. 15, 1745–1752.
Jin, M., Kumar, A., Kumar, S., 2012. Ethanol-mediated regulation of cytochrome P450 2A6 expression in monocytes: role of oxidative stress-mediated PKC/MEK/Nrf2 pathway. PLoS One 7, e35505.
Kaul, S., Anantharam, V., Yang, Y., Choi, C.J., Kanthasamy, A., Kanthasamy, A.G., 2005. Tyrosine phosphorylation regulates the proteolytic activation of protein kinase Cδ in dopaminergic neuronal cells. J. Biol. Chem. 280, 28721–28730.
Kim, S.G., Cho, J.Y., Chung, Y.S., Ahn, E.T., Lee, K.Y., Han, Y.B., 1998. Suppression of xenobiotic-metabolizing enzyme expression in rats by acriflavine, a protein kinase C inhibitor. Effects on epoxide hydrolase, glutathione S-transferases, and cytochromes p450. Drug Metab. Dispos. 26, 66–72.
Krasnova, I.N., Cadet, J.L., 2009. Methamphetamine toxicity and messengers of death. Brain Res. Rev. 60, 379–407.
Liu, M., Sun, A., Shin, E.J., Liu, X., Kim, S.G., Runyons, C.R., Markesbery, W., Kim, H.C., Bing, G., 2006. Expression of microsomal epoxide hydrolase is elevated in Alzheimer's hippocampus and induced by exogenous beta-amyloid and trimethyl-tin. Eur. J. Neurosci. 23, 2027–2034.
Liu, M., Hunter, R., Nguyen, X.V., Kim, H.C., Bing, G., 2008. Microsomal epoxide hydrolase deletion enhances tyrosine hydroxylase phosphorylation in mice after MPTP treatment. J. Neurosci. Res. 86, 2792–2801.
Liu, B., Traini, R., Killinger, B., Schneider, B., Moszczynska, A., 2013. Overexpression of parkin in the rat nigrostriatal dopamine system protects against methamphetamine neurotoxicity. Exp. Neurol. 247, 359–372.
Mai, H.N., Sharma, N., Shin, E.J., Nguyen, B.T., Nguyen, P.T., Jeong, J.H., Cho, E.H., Lee, Y.J., Kim, N.H., Jang, C.G., Nabeshima, T., Kim, H.C., 2018a. Exposure to far-infrared ray attenuates methamphetamine-induced impairment in recognition memory through inhibition of protein kinase Cδ in male mice: comparison with the antipsychotic clozapine. J. Neurosci. Res. 96, 1294–1310.
Mai, H.N., Sharma, N., Shin, E.J., Nguyen, B.T., Nguyen, P.T., Jeong, J.H., Jang, C.G., Cho, E.H., Nah, S.Y., Kim, N.H., Nabeshima, T., Kim, H.C., 2018b. Exposure to far-infrared rays attenuates methamphetamine-induced recognition memory impairment via modulation of the muscarinic M1 receptor, Nrf2, and PKC. Neurochem. Int. 116, 63–76.
Mai, H.N., Jung, T.W., Kim, D.J., Sharma, G., Sharma, N., Shin, E.J., Jang, C.G., Nah, S.Y., Lee, S.H., Chung, Y.H., Lei, X.G., Jeong, J.H., Kim, H.C., 2018c. Protective potential of glutathione peroxidase-1 gene against cocaine-induced acute hepatotoxic consequences in mice. J. Appl. Toxicol. 38, 1502–1520.
Mai, H.N., Lee, S.H., Sharma, G., Kim, D.J., Sharma, N., Shin, E.J., Pham, D.T., Trinh, Q.D., Jang, C.G., Nah, S.Y., Jeong, J.H., Kim, H.C., 2019a. Protein kinase Cδ knockout mice are protected from cocaine-induced hepatotoxicity. Chem. Biol. Interact. 297, 95–108.
Mai, H.N., Nguyen, L.T.T., Shin, E.J., Kim, D.J., Jeong, J.H., Chung, Y.H., Lei, X.G., Sharma, N., Jang, C.G., Nabeshima, T., Kim, H.C., 2019b. Astrocytic mobilization of glutathione peroxidase-1 contributes to the protective potential against cocaine kindling behaviors in mice via activation of JAK2/STAT3 signaling. Free Radic. Biol. Med. 131, 408–431.
Mai, H.N., Sharma, N., Jeong, J.H., Shin, E.J., Pham, D.T., Trinh, Q.D., Lee, Y.J., Jang, C.G., Nah, S.Y., Bing, G., Kim, H.C., 2019c. P53 knockout mice are protected from cocaine-induced kindling behaviors via inhibiting mitochondrial oxidative burdens, mitochondrial dysfunction, and proapoptotic changes. Neurochem. Int. 124, 68–81.
Melnick, R.L., 2002. Carcinogenicity and mechanistic insights on the behavior of epoxides and epoxide-forming chemicals. Ann. N. Y. Acad. Sci. 982, 177–189.
Miyamoto, A., Nakayama, K., Imaki, H., Hirose, S., Jiang, Y., Abe, M., Tsukiyama, T., Nagahama, H., Ohno, S., Hatakeyama, S., Nakayama, K.I., 2002. Increased proliferation of B cells and auto-immunity in mice lacking protein kinase Cδ. Nature 416, 865–869.
Miyata, M., Kudo, G., Lee, Y.H., Yang, T.J., Gelboin, H.V., Fernandez-Salguero, P., Kimura, S., Gonzalez, F.J., 1999. Targeted disruption of the microsomal epoxide hydrolase gene. Microsomal epoxide hydrolase is required for the carcinogenic activity of 7,12-dimethylbenz[a]anthracene. J. Biol. Chem. 274, 23963–23968.
Naik, M.U., Benedikz, E., Hernandez, I., Libien, J., Hrabe, J., Valsamis, M., Dow-Edwards, D., Osman, M., Sacktor, T.C., 2000. Distribution of protein kinase Mzeta and the complete protein kinase C isoform family in rat brain. J. Comp. Neurol. 426, 243–258.
Nguyen, X.K., Lee, J., Shin, E.J., Dang, D.K., Jeong, J.H., Nguyen, T.T., Nam, Y., Cho, H.J., Lee, J.C., Park, D.H., Jang, C.G., Hong, J.S., Nabeshima, T., Kim, H.C., 2015. Liposomal melatonin rescues methamphetamine-elicited mitochondrial burdens, proapoptosis, and dopaminergic degeneration through the inhibition PKCδ gene. J. Pineal Res. 58, 86–106.
Nguyen, P.T., Shin, E.J., Dang, D.K., Tran, H.Q., Jang, C.G., Jeong, J.H., Lee, Y.J., Lee, H.J., Lee, Y.S., Yamada, K., Nabeshima, T., Kim, H.C., 2018. Role of dopamine D1 receptor in 3-fluoromethamphetamine-induced neurotoxicity in mice. Neurochem. Int. 113, 69–84.
Omiecinski, C.J., Hassett, C., Hosagrahara, V., 2000. Epoxide hydrolase–polymorphism and role in toxicology. Toxicol. Lett. 112–113, 365–370.
Omonijo, O., Wongprayoon, P., Ladenheim, B., McCoy, M.T., Govitrapong, P., Jayanthi, S., Cadet, J.L., 2014. Differential effects of binge methamphetamine injections on the mRNA expression of histone deacetylases (HDACs) in the rat striatum. Neurotoxicology 45, 178–184.
Orjuela Leon, A.C., Marwosky, A., Arand, M., 2017. Evidence for a complex formation between CYP2J5 and mEH in living cells by FRET analysis of membrane protein interaction in the endoplasmic reticulum (FAMPIR). Arch. Toxicol. 91, 3561–3570.
Park, J.H., Gopishetty, S., Szewczuk, L.M., Troxel, A.B., Harvey, R.G., Penning, T.M., 2005. Formation of 8-oxo-7,8-dihydro-2'-deoxyguanosine (8-oxo-dGuo) by PAH o-quinones: involvement of reactive oxygen species and copper(II)/copper(I) redox cycling. Chem. Res. Toxicol. 18, 1026–1037.
Riddle, E.L., Fleckenstein, A.E., Hanson, G.R., 2006. Mechanisms of methamphetamine-induced dopaminergic neurotoxicity. AAPS J. 8, E413–E418.
Roseboom, P.H., Namboodiri, M.A., Zimonjic, D.B., Popescu, N.C., Rodriguez, I.R., Gastel, J.A., Klein, D.C., 1998. Natural melatonin 'knockdown' in C57BL/6J mice: rare mechanism truncates serotonin N-acetyltransferase. Brain Res. Mol. Brain Res. 63, 189–197.
Shahid, A., Ali, R., Ali, N., Hasan, S.K., Bernwal, P., Afzal, S.M., Vafa, A., Sultana, S., 2016. Modulatory effects of catechin hydrate against genotoxicity, oxidative stress, inflammation and apoptosis induced by benzo(a)pyrene in mice. Food Chem. Toxicol. 92, 64–74.
Shin, E.J., Bing, G., Chae, J.S., Kim, T.W., Bach, J.H., Park, D.H., Yamada, K., Nabeshima, T., Kim, H.C., 2009. Role of microsomal epoxide hydrolase in methamphetamine-induced drug dependence in mice. J. Neurosci. Res. 87, 3679–3686.
Shin, E.J., Duong, C.X., Nguyen, X.T., Bing, G., Bach, J.H., Park, D.H., Nakayama, K., Ali, S.F., Kanthasamy, A.G., Cadet, J.L., Nabeshima, T., Kim, H.C., 2011. PKCδ inhibition enhances tyrosine hydroxylase phosphorylation in mice after methamphetamine treatment. Neurochem. Int. 59, 39–50.
Shin, E.J., Duong, C.X., Nguyen, X.T., Li, Z., Bing, G., Bach, J.H., Park, D.H., Nakayama, K., Ali, S.F., Kanthasamy, A.G., Cadet, J.L., Nabeshima, T., Kim, H.C., 2012. Role of oxidative stress in methamphetamine-induced dopaminergic toxicity mediated by protein kinase Cδ. Behav. Brain Res. 232, 98–113.
Shin, E.J., Shin, S.W., Nguyen, T.T., Park, D.H., Wie, M.B., Jang, C.G., Nah, S.Y., Yang, B.W., Ko, S.K., Nabeshima, T., Kim, H.C., 2014. Ginsenoside Re rescues methamphetamine-induced oxidative damage, mitochondrial dysfunction, microglial activation, and dopaminergic degeneration by inhibiting the protein kinase Cδ gene. Mol. Neurobiol. 49, 1400–1421.
Shin, E.J., Dang, D.K., Tran, H.Q., Nam, Y., Jeong, J.H., Lee, Y.H., Park, K.T., Lee, Y.S., Jang, C.G., Hong, J.S., Nabeshima, T., Kim, H.C., 2016. PKCδ knockout mice are protected from para-methoxymethamphetamine-induced mitochondrial stress and associated neurotoxicity in the striatum of mice. Neurochem. Int. 100, 146–158.
Shin, E.J., Dang, D.K., Tran, T.V., Tran, H.Q., Jeong, J.H., Nah, S.Y., Jang, C.G., Yamada, K., Nabeshima, T., Kim, H.C., 2017. Current understanding of methamphetamine-associated dopaminergic neurodegeneration and psychotoxic behaviors. Arch. Pharm. Res. 40, 403–428.
Shin, E.J., Hwang, Y.G., Sharma, N., Tran, H.Q., Dang, D.K., Jang, C.G., Jeong, J.H., Nah, S.Y., Nabeshima, T., Kim, H.C., 2018a. Role of protein kinase Cδ in dopaminergic neurotoxic events. Food Chem. Toxicol. 121, 254–261.
Shin, E.J., Tran, H.Q., Nguyen, P.T., Jeong, J.H., Nah, S.Y., Jang, C.G., Nabeshima, T., Kim, H.C., 2018b. Role of mitochondria in methamphetamine-induced dopaminergic neurotoxicity: involvement in oxidative stress, neuroinflammation, and pro-apoptosis-A review. Neurochem. Res. 43, 66–78.
Shin, E.J., Dang, D.K., Hwang, Y.G., Tran, H.Q., Sharma, N., Jeong, J.H., Jang, C.G., Nah, S.Y., Nabeshima, T., Yoneda, Y., Cadet, J.L., Kim, H.C., 2019. Significance of protein kinase C in the neuropsychotoxicity induced by methamphetamine-like psychostimulants. Neurochem. Int. 124, 162–170.
Springer, L.N., Tilly, J.L., Sipes, I.G., Hoyer, P.B., 1996. Enhanced expression of bax in small preantral follicles during 4-vinylcyclohexene diepoxide-induced ovotoxicity in the rat. Toxicol. Appl. Pharmacol. 139, 402–410.
Srivastava, D., 2016. Microsomal epoxide hydrolase gene polymorphisms and susceptibility to prostate cancer: a systematic review. Indian J. Cancer 53, 213–215.
Thrash-Williams, B., Karuppagounder, S.S., Bhattacharya, D., Ahuja, M., Suppiramaniam, V., Dhanasekaran, M., 2016. Methamphetamine-induced dopaminergic toxicity prevented owing to the neuroprotective effects of salicylic acid. Life Sci. 154, 24–29.
Tran, H.Q., Lee, Y., Shin, E.J., Jang, C.G., Jeong, J.H., Mouri, A., Saito, K., Nabeshima, T., Kim, H.C., 2018a. PKCδ knockout mice are protected from dextromethorphan-induced serotonergic behaviors in mice: involvements of downregulation of 5-HT1A receptor and upregulation of Nrf2-dependent GSH synthesis. Mol. Neurobiol. 55, 7802–7821.
Tran, T.-V., Shin, E.-J., Nguyen, L.T.T., Lee, Y., Kim, D.-J., Jeong, J.H., Jang, C.-G., Nah, S.-Y., Toriumi, K., Nabeshima, T., Yamada, K., Kim, H.-C., 2018b. Protein kinase Cδ gene depletion protects against methamphetamine-induced impairments in recognition memory and ERK1/2 signaling via upregulation of glutathione peroxidase-1 gene. Mol. Neurobiol. 55, 4136–4159.
Tran, H.Q., Shin, E.J., Hoai Nguyen, B.C., Phan, D.H., Kang, M.J., Jang, C.G., Jeong, J.H., Nah, S.Y., Mouri, A., Saito, K., Nabeshima, T., Kim, H.C., 2019. 5-HT1A receptor agonist 8-OH-DPAT induces serotonergic behaviors in mice via interaction between PKCδ and p47phox. Food Chem. Toxicol. 123, 125–141.
Vilgrain, I., Defaye, G., Chambaz, E.M., 1984. Adrenocortical cytochrome P-450 responsible for cholesterol side chain cleavage (P-450scc) is phosphorylated by the calcium-activated, phospholipid-sensitive protein kinase (protein kinase C). Biochem. Biophys. Res. Commun. 125, 554–561.
Xie, T., McCann, U.D., Kim, S., Yuan, J., Ricaurte, G.A., 2000. Effect of temperature on dopamine transporter function and intracellular accumulation of methamphetamine: implications for methamphetamine-induced dopaminergic neurotoxicity. J. Neurosci.

20, 7838–7845.
Yoshida, K., 2007. PKCδ signaling: mechanisms of DNA damage response and apoptosis. Cell. Signal. 19, 892–901.
Yu, L., Cherng, C.F., Chen, C., 2002. Melatonin in concentrated ethanol and ethanol alone attenuate methamphetamine-induced dopamine depletions in C57BL/6J mice. J. Neural Transm. 109, 1477–1490.
Zhang, D., Anantharam, V., Kanthasamy, A., Kanthasamy, A.G., 2007a. Neuroprotective effect of protein kinase Cδ inhibitor rottlerin in cell culture and animal models of Parkinson's disease. J. Pharmacol. Exp. Ther. 322, 913–922.
Zhang, D., Kanthasamy, A., Yang, Y., Anantharam, V., Kanthasamy, A., 2007b. Protein kinase C delta negatively regulates tyrosine hydroxylase activity and dopamine synthesis by enhancing protein phosphatase-2A activity in dopaminergic neurons. J. Neurosci. 27, 5349–5362.